Molecular Biotechnology
https://doi.org/10.1007/s12033-023-00953-2

ORIGINAL PAPER

METTL3 Mediated MALAT1 m6A Modification Promotes Proliferation and Metastasis in Osteosarcoma Cells

Yuanzhuang Zhang[1] · Yeqiu Xu[1] · Guanzhen Qiu[1] · Yinzhou Luo[1] · Yuxin Bao[1] · Jie Lu[2] · Tao Wang[1] · Yong Wang[1]

Received: 3 April 2023 / Accepted: 16 October 2023

Abstract

Background As one of the most ubiquitous types of posttranscriptional modification, N6-methyladenosine (m6A) is extensively implicated in almost all types of cancers, including osteosarcoma. Our previous research partially uncovered the role of Metastasis Associated Lung Adenocarcinoma Transcript 1 (MALAT1) in osteosarcoma. However, the relationships between methyltransferase-like 3 (METTL3) and noncoding RNAs modified by METTL3, especially MALAT1, in osteosarcoma remain obscure.

Methods The expression of METTL3 in osteosarcoma was evaluated by online bioinformatics analysis, immunohistochemical (IHC) staining, western blotting (WB), and reverse transcription–quantitative PCR (RT–qPCR). Cell Counting Kit 8 (CCK-8) and Transwell assays were used to evaluate the cell proliferation and invasion abilities. The expression of MALAT1 in osteosarcoma was evaluated by online bioinformatics analysis and RT–qPCR analysis. m6A methylated RNA immunoprecipitation-qPCR (MeRIP-qPCR) was used to detect m6A modification changes in MALAT1. An actinomycin D assay was used to study changes in the stability of MALAT1.

Results METTL3 was upregulated in osteosarcoma tissues and cell lines. Functionally, METTL3 promoted the proliferation and migration of osteosarcoma cells. Moreover, a clear positive correlation was found between METTL3 and MALAT1 expression, and MALAT1 was upregulated in osteosarcoma tissues and cells. Mechanistically, the presence of m6A modification sites in MALAT1 and METTL3-mediated m6A modification increased the stability of MALAT1 in osteosarcoma cells and promoted their proliferation and migration.

Conclusion In this study, it was concluded that in osteosarcoma cells, METTL3, acting as an oncogene, promoted m6A modification of MALAT1, increased the stability of MALAT, and enhanced MALAT1-mediated oncogenic function.

Keywords Osteosarcoma · METTL3 · m6A · MALAT1 · Proliferation · Migration

✉ Tao Wang
wtzxj2018@163.com

✉ Yong Wang
wy_zju@hotmail.com

Yuanzhuang Zhang
zhangyuanzhuang@126.com

Yeqiu Xu
xuyeqiu0830@hotmail.com

Guanzhen Qiu
13464104601@163.com

Yinzhou Luo
18041368300@163.com

Yuxin Bao
baoyuxin0320@163.com

Jie Lu
lujie0625@163.com

[1] Fourth Department of Orthopedic Surgery, Central Hospital Affiliated to Shenyang Medical College, No. 5 South Seven West Road, Tiexi, Shenyang 110024, Liaoning, P.R. China

[2] Department of Cardiology, Shenyang Fourth People's Hospital, China Medical University, Shenyang 110031, Liaoning, P.R. China

Published online: 28 October 2023

Introduction

Osteosarcoma, a term first proposed in 1805 by the French surgeon Alexis Boyer, refers to a tumor derived from primitive osteogenic mesenchymal cells and describes the production of bone by osteosarcoma cells [1]. As the most common and aggressive type of bone neoplasm in children and adolescents, osteosarcoma frequently occurs in the epiphyses of long bones; therefore, osteosarcoma is characterized by rapid growth and fast progression [2]. Currently, despite substantial advances in osteosarcoma treatment strategies, including surgical excision and neoadjuvant or adjuvant chemotherapy and radiotherapy, the 5-year survival rate of osteosarcoma remains low, and recurrence and metastasis remain particularly common [3]. A deeper exploration of the underlying molecular mechanisms of osteosarcoma is therefore of great importance.

m6A modification is present in most RNA species, including messenger RNAs (mRNAs), long noncoding RNAs (lncRNAs), ribosomal RNAs (rRNAs), transfer RNAs (tRNAs), and small nuclear RNAs (snRNAs) [4]. More than 12,000 m6A sites have been found in more than 7000 human genes, which are rich in RRACH (R = G or A, H = A, C or U) shared sequences. These sequences are usually located in the termination codon and 3′ untranslated region (3′UTR) [5, 6]. Methyltransferase-like 3 (METTL3), a 70 kDa protein, was the first identified m6A methyltransferase, and METTL3 is highly conserved in eukaryotes from yeast to humans [7]. METTL3 is widely involved in various malignancies through its action as either an oncogene or a tumor suppressor [8]. In osteosarcoma, previous studies have focused on mRNAs, such as ATPase family AAA domain containing 2 (ATAD2), developmentally regulated GTP binding protein 1 (DRG1), TNF receptor-associated factor 6 (TRAF6), CCR4-NOT transcription complex subunit 7 m (CONT7) and tripartite motif containing 7 (TRIM7), as the targets of METTL3 [9–13]. However, there are few studies on the involvement of METTL3-modified lncRNAs in osteosarcoma progression. METTL3 was revealed to increase the stability of DANCR and promote DANCR-mediated malignant progression of osteosarcoma in an m6A-dependent manner [14]. However, the interaction between METTL3 and Metastasis Associated Lung Adenocarcinoma Transcript 1 (MALAT1), a well-known oncogenic lncRNA, in osteosarcoma remains obscure.

As a highly studied oncogenic lncRNA, MALAT1 is evolutionarily conserved between humans and other species. The MALAT1 sequence, approximately 8.7 kb in length, is located on human chromosome 11q13.1 [15]. MALAT1 is widely involved in multiple neoplastic diseases, including lung cancer, breast cancer, liver cancer, colorectal cancer, and osteosarcoma [16]. It has been found that high levels of MALAT1 mediate osteosarcoma cell growth and tumorigenicity through targeting of different signaling pathways and miRNAs [15]. In our previous research, we showed that MALAT1 was upregulated in osteosarcoma. Additionally, we demonstrated that MALAT1 promoted osteosarcoma cell proliferation and migration via upregulation of Rho associated coiled-coil containing protein kinase 1 (ROCK1) by sponging miR-144-3p [17]. It was reported that certain m6A regulators, for example, Fat mass and obesity-associated (FTO) and Methyltransferase-like 14 (METTL14), interact with MALAT1 and affect its level via diverse mechanisms [18, 19]. However, the interaction between METTL3 and MALAT1 in osteosarcoma remains unclear.

The present study first investigated the association of METTL3-mediated m6A modification and MALAT1 in osteosarcoma. The current study aimed to uncover the role of the METTL3/MALAT1 axis in osteosarcoma from a novel perspective.

Materials and Methods

Patients and Tissue Samples

Tissue samples from five patients with osteosarcoma and the corresponding paratumor tissue samples were collected in this study, and all samples were surgically resected under aseptic conditions, washed in saline, and stored in liquid nitrogen for further study. The Medical Ethics Committee of Central Hospital Affiliated with Shenyang Medical College approved this study (approval number: 2019DEC12-4), and all patients provided written informed consent.

Cell Culture

hFOB1.19 normal osteoblasts as well as MG-63 and U2OS osteosarcoma cells were obtained from the Cell Bank of the Chinese Academy of Sciences (Shanghai, China). hFOB1.19 cells were cultured using DMEM/F12 medium (Gibco, El Paso, TX, USA), MG-63 cells were cultured using DMEM (Gibco), and U2OS cells were cultured using MEM (Gibco). All media were supplemented with 10% (v/v) fetal bovine serum (FBS, Gibco) as well as penicillin/streptomycin solution (penicillin concentration: 100 U/ml, streptomycin concentration: 0.1 mg/ml) (Beijing Solarbio Science & Technology Co., Ltd., Beijing, China). hFOB1.19 cells were cultured in a cell culture incubator at 34 °C in 5% CO_2, while MG-63 and U2OS cells were cultured in a cell culture incubator at 37 °C in 5% CO_2.

Immunohistochemical (IHC) Staining

Immunohistochemical staining of osteosarcoma tissue was performed according to previous descriptions [20]. Osteosarcoma tissue specimens were sequentially fixed with 4% paraformaldehyde (Servicebio, Wuhan, China), embedded in paraffin, sectioned at a 4 μm thickness, dewaxed, rehydrated, blocked with 3% hydrogen peroxide, and blocked with 10% goat serum. The sections were then incubated with primary antibodies against METTL3 (dilution, 1:500; cat. no. ab195352; Abcam) at 4 °C overnight. On the second day, the sections were incubated with the secondary antibody (goat anti-rabbit immunoglobulin G HRP-conjugated; cat. no. ab205718; dilution 1:10,000; Abcam) for 50 min, after which a streptavidin-horseradish peroxidase complex was added. Then, DAB chromogenic solution (Servicebio) was added, and the sections were incubated for 5 min, rinsed with tap water, stained with hematoxylin (Servicebio) for 3 min, incubated with hematoxylin differentiation solution for 3 s, incubated with hematoxylin bluing solution to restore the blue color, and rinsed with running water. Afterward, the samples were dehydrated under a series of concentrations of alcohol, sealed with drops of rhamsan gum (Servicebio), and placed under a microscope (Olympus) for observation.

Western Blotting

The method of this experiment has been described in detail before [21]. RIPA lysis buffer (Servicebio) was added to the collected osteosarcoma cells and tissues for lysis, the supernatant was collected by high-speed centrifugation at 4 °C, and the protein concentration was measured with a BCA Protein Assay Kit (Servicebio). Then, the proteins were separated by 10% SDS–PAGE and transferred to polyvinylidene difluoride (PVDF) membranes (Servicebio), which were blocked with rapid blocking solution (New Cell & Molecular Biotech. Ltd., Suzhou, China) for 10 min and then incubated with primary antibodies against METTL3 (dilution, 1:1000; cat. no. ab195352; Abcam) and GAPDH (dilution, 1:10,000; cat. no. ab181602; Abcam) at 4 °C overnight. Unbound antibody was removed by washing with TBST. The secondary antibody (goat anti-rabbit immunoglobulin G HRP-conjugated; cat. no. ab205718; dilution 1:10,000; Abcam) was added for incubation at room temperature for one hour and was then removed by washing with TBST. Finally, immunoreactions were visualized using a Hypersensitivity ECL Chemiluminescence Detection Kit (Sevenbio, Beijing, China). Protein signals were visualized with a gel imager (ChemiScope6100, Clinx Science Instruments Co., Ltd., Shanghai, China).

Table 1 Primer and oligonucleotide sequences used in the present research

Primers	**Sequences (5'-3')**
METTL3 forward	TTGTCTCCAACCTTCCGTAGT
METTL3 reverse	CCAGATCAGAGAGGTGGTGTAG
MALAT1 forward	CATTCGCTTAGTTGGTCTAC
MALAT1 reverse	TTCTACCGTTTTTAGCTTC
GAPDH forward	CAAGGTCATCCATGACAACTTTG
GAPDH reverse	GTCCACCACCCTGTTGCTGTAG
Oligonucleotide	**Sequences (5'-3')**
siMETTL3-1	CTGCAAGTATGTTCACTATGA
siMETTL3-2	CGTCAGTATCTTGGGCAAGTT
siMALAT1-1	GAGCAAAGGAAGTGGCTTA
siMALAT1-2	TCTTCAAGAGAGATATTTAA
siSCR	UUCUCCGAACGUGUCACGU dTdT

RNA Extraction and Reverse Transcription–quantitative PCR (RT–qPCR)

RT–qPCR analyses were performed as previously described [22]. Total RNA from osteosarcoma tissues and cells was extracted using the TRIzol kit (Invitrogen). Primers were synthesized by TaKaRa (TaKaRa Bio Inc., Beijing, China), and primer sequences are listed in Table 1. The PrimeScript™ RT Master Mix Reagent Kit (TaKaRa, Beijing, China) was used to reverse transcribe the extracted RNA into first-strand cDNA. The TB Green® Premix Ex Taq™ II Reagent Kit (TaKaRa) was used to amplify cDNA. GAPDH was used as an internal control. Relative expression was determined by the $2^{-\Delta\Delta CT}$ method.

Oligonucleotide and Plasmid Transfection

GenePharma (Shanghai, China) designed and synthesized two specific small interfering RNA against METTL3 (si-METTL3-1 and siMETTL3-2), two specific small interfering RNA against MALAT1 (si-MALAT1-1 and si-MALAT1-2), and the corresponding blank control scrambled siRNA (siSCR). The METTL3 overexpression plasmid (oeMETTL3) and MALAT1 overexpression plasmid (oeMALAT1) were similarly designed and synthesized by GenePharma. Overexpression plasmids were transfected using the Lipofectamine 3000 kit (Invitrogen, Carlsbad, CA, USA). si-METTL3-1, siMETTL3-2, siMALAT1-1, siMALAT1-2, and siSCR were transfected into MG-63 and U2OS cells according to the riboFect ™ CP Transfer Kit (RiboBio, Guangzhou, China) instructions. oeMETTL3, oeMALAT1, and the corresponding blank vector pcDNA were transfected into MG-63 and U2OS cells according to the instructions of the Lipofectamine 3000 kit (Invitrogen). The sequences of the siRNAs are listed in Table 1.

Cell Counting Kit-8 (CCK8) Assay

MG-63 and U2OS cell viability was assayed using the CCK8 kit (Servicebio) as previously reported [23]. After gene overexpression or silencing in osteosarcoma cells, the cells were seeded in 96-well plates at a density of 2000 cells in 100 µl per well and incubated overnight in an incubator at 37 °C under 5% CO_2. On Days 1, 2, 3, and 4, 10 µL of CCK8 solution was added to each well of the 96-well plates, which were placed in the incubator for 2 h. Afterward, the cells were analyzed by measuring the optical density at 450 nm in a microplate reader (Bio-Rad, Hercules, CA, USA).

Transwell Assay

The Transwell assay procedures were performed as previously reported [24]. A total of 1×10^5 osteosarcoma cells were spread into Transwell chambers, 2 ml of serum-free medium was added, and 700 µL of complete medium with serum was added to a 24-well plate. The chambers were placed into the 24-well plate and cultured for 24 h in an incubator at 37 °C with 5% CO_2. After removing the Transwell chambers, the chambers were washed with PBS, the cells on the chamber membrane that had not passed through the membrane were removed by wiping with a cotton swab, and the chambers were washed again with PBS. Immediately after that, the cells remaining in the chambers were fixed with methanol for 20 min, washed with PBS, stained in 0.1% crystal violet staining solution (Servicebio) for 30 min, and rinsed with running water. Finally, the rinsed chambers were placed under a microscope (Olympus, Tokyo, Japan) for observation and imaging.

m6A Methylated RNA Immunoprecipitation-qPCR (MeRIP-qPCR)

MeRIP-qPCR assays were performed to determine the m6A level of MALAT1 according to the instructions of the BersinBioTM m6A MeRIP kit (BersinBio, Guangzhou, China) [25]. RNA extraction was performed using the method described above. Fragmentation buffer was added to the collected RNA samples and incubated at 94 °C for 2 min to fragment the RNA, after which IP buffer 1 and an RNase inhibitor were added to solubilize the RNA samples. 10% of each sample was stored as the input group, and the remaining portions of the samples were used as the IP group for immunoprecipitation. IP buffer 2 was added to the samples in the IP group, an anti-m6A antibody (dilution, 1:500; cat. no. ab151230; Abcam) or IgG (dilution, 1:100; cat. no. ab109489; Abcam) was then added, and the samples were incubated in a vertical mixer at 4 °C for 4 h. Protein A/G beads were washed with IP buffer, blocked with BSA, and then added to the samples in the IP group prior to incubation in a vertical mixer at 4 °C for 2 h. RNA was eluted using elution buffer, and protease K was added for digestion at 55 °C for 30 min. The eluted RNA fragments were recovered and purified using the GeneJET RNA Purification Kit (Thermo Fisher Scientific, USA), and RNA enrichment was analyzed by RT–qPCR.

RNA Stability Assay

To determine the stability of MALAT1, an actinomycin D assay was performed as previously described [26]. A total of 3×10^5 cells were resuspended, seeded in 6-well plates and incubated at 37 °C in 5% CO_2 for 24 h. Then, the osteosarcoma cells were treated with 2 µg/ml actinomycin D (Sigma, St. Louis, MO, USA), and total RNA was extracted at 0 h, 3 h, and 6 h. The expression of MALAT1 was measured by RT–qPCR.

Bioinformatics Analysis

To analyze the expression of METTL3 in osteosarcoma in the GEO database, the data from osteosarcoma-related dataset GSE42352 (https://www.ncbi.nlm.nih.gov/geo/query/acc.cgi?acc=GSE42352) were analyzed with the online tool GEO2R [27] of the GEO database; the corresponding probe ID was cefr67QKA1UKfQUq3o. According to the instructions on the website, the expression of METTL3 in TCGA was analyzed using the online tool UALCAN [28, 29], and the correlation between METTL3 and MALAT1 expression in TCGA was analyzed using the online tool GEPIA2 [30]. The online software SRAMP [31] and the RMBase database (version 2.0) [32] were used to predict the theoretical m6A modification sites in MALAT1 (RefSeq ID: NR_002819.4).

Statistical Analysis

The obtained data were statistically analyzed using GraphPad Prism 7.0. Data from the studies are shown as the means ± standard deviations; the expression of METTL3 and MALAT1 was compared at the osteosarcoma tissue level using paired t tests and at the osteosarcoma cell level by one-way ANOVA. * represents $P<0.05$, ** represents $P<0.01$, *** represents $P<0.001$, **** represents $P<0.0001$, and significant differences were assumed when the P value was <0.05.

Results

METTL3 is Upregulated in Osteosarcoma Tissues and Cell Lines

We collected tissue samples from five patients with osteosarcoma and checked the expression of METTL3 in osteosarcoma tissues and the corresponding paratumor tissues by IHC staining, and the results showed that METTL3 expression was higher in osteosarcoma tissues than in paratumor tissues (Fig. 1a). Next, we examined the expression of METTL3 in the abovementioned five pairs of osteosarcoma tissue samples by western blot analysis, and the results were similar to those of the IHC assay, further indicating that METTL3 expression is obviously higher in osteosarcoma tissues (Fig. 1b). We next focused on METTL3 expression in osteosarcoma-related data in the GEO and TCGA databases. We analyzed the expression of METTL3 in non-osteosarcoma samples (15 cases) and osteosarcoma samples (103 cases) in the GSE42352 dataset (Fig. 1c), and the expression of METTL3 in osteosarcoma samples was found to be significantly higher than that in non-osteosarcoma samples. In the TCGA database, METTL3 had higher expression in the sarcoma primary tumor group (260 cases) than in the normal group (2 cases) (Fig. 1d). We examined the differences in the METTL3 expression levels in hFOB 1.19 normal osteoblasts and MG-63 and U2OS osteosarcoma cells by RT–qPCR and Western blotting. The findings demonstrated that the expression levels of METTL3 mRNA and protein were obviously higher in MG-63 and U2OS cells than in hFOB 1.19 cells (Fig. 1-f). Collectively, the above findings indicated that METTL3 might be a potential biomarker for osteosarcoma.

METTL3 Promotes Proliferation and Migration in MG-63 and U2OS Cells

We then investigated the roles of METTL3 in cell proliferation and metastasis in MG-63 and U2OS cells. We transfected siMETTL3-1 and siMETTL3-2 and a siSCR as well

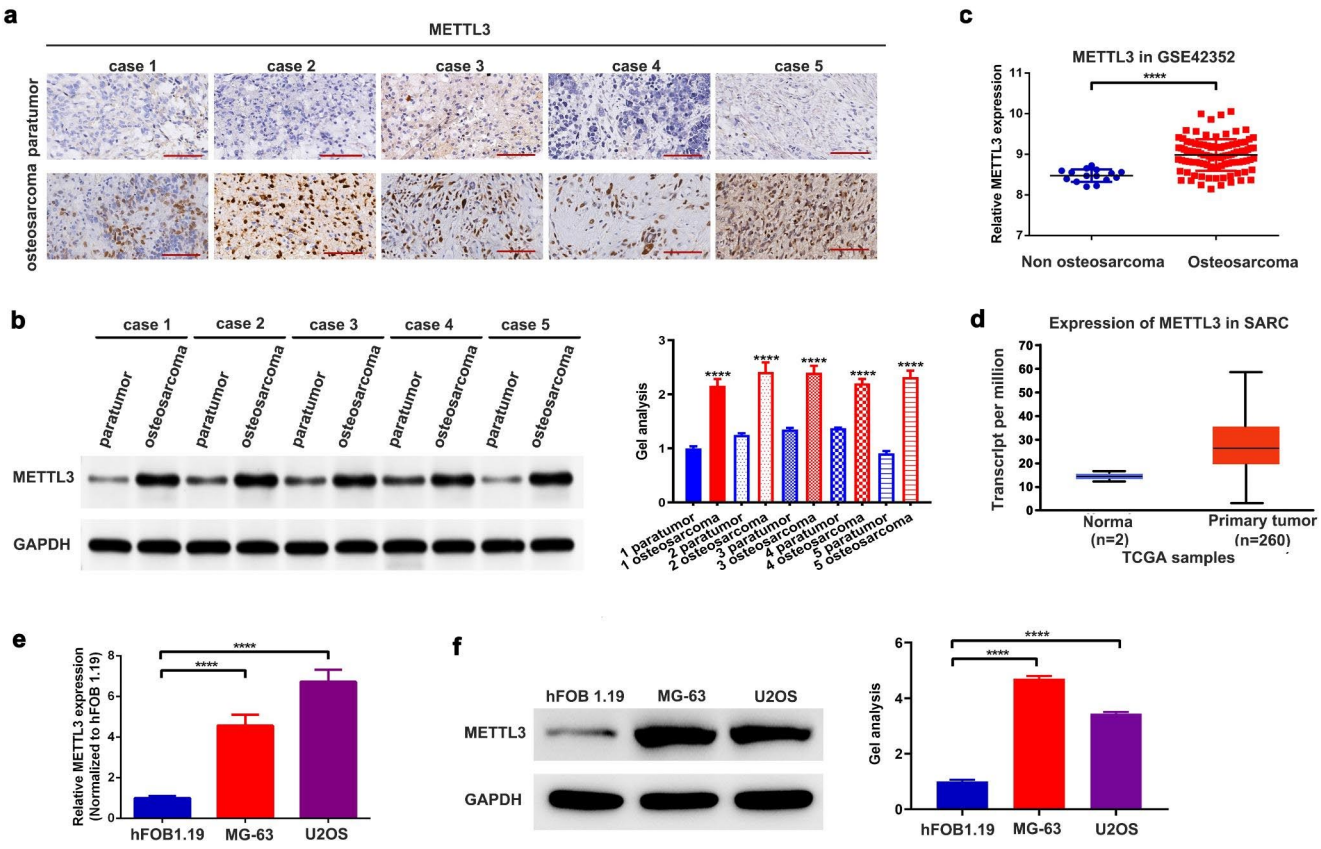

Fig. 1 METTL3 is upregulated in osteosarcoma tissues and cell lines. (a-b) The expression of METTL3 in 5 osteosarcoma and paratumor tissues was measured by an IHC assay (a) and western blot analysis (b). Magnification: 400×; Scale bar: 50 μm. $^{****}P < 0.0001$ compared with the paratumor group. (c) The expression of METTL3 in 15 non-osteosarcoma tissues and 103 osteosarcoma tissues according to online analysis of the OS-related GEO dataset GSE42352 by using GEO2R. $^{****}P < 0.0001$ compared with non-osteosarcoma tissues. (d) The expression of METTL3 in 2 normal tissues and in 260 sarcoma tissues was analyzed with the online UALCAN tool. $^{*}P < 0.05$ compared with normal tissues. (e-f) The expression of METTL3 in the normal human osteoblast cell line hFOB1.19 and in two osteosarcoma cell lines, MG-63 and U2OS, was measured by RT–qPCR analysis (e) and western blot analysis (f). $^{****}P < 0.0001$ compared with hFOB 1.19

as the oeMETTL3 and the pcDNA into MG-63 and U2OS cells. METTL3 expression was measured by RT–qPCR and Western blotting, and the results are presented in Fig. 2a-b. The expression levels of METTL3 in MG-63 and U2OS cells were decreased after transfection with siMETTL3-1 and siMETTL3-2. After transfection with oeMETTL3, the level of METTL3 in MG-63 and U2OS cells was increased, confirming the successful construction of our cell model. We further investigated the impact of different METTL3 expression levels on the proliferation and migration abilities of MG-63 and U2OS osteosarcoma cells by a CCK8 assay and a Transwell assay, and the results are presented in Fig. 2c-d. The proliferation and migration of MG-63 and U2OS osteosarcoma cells were also markedly inhibited after transfection with siMETTL3-1 and siMETTL3-2 compared to the siSCR. In contrast, after transfection of oeMETTL3, MG-63 and U2OS cells exhibited significantly increased proliferation and migration abilities.

MALAT1 Expression is Upregulated and is Positively Correlated with METTL3 Expression in Osteosarcoma

Via online analysis of the TCGA database via GEPIA2 [30], we discovered that METTL3 expression was significantly and positively correlated with MALAT1 expression (Fig. 3a). We then examined the differential expression of MALAT1 in five pairs of collected osteosarcoma samples and the corresponding paratumor tissue samples by RT–qPCR. The results showed that MALAT1 had a higher expression level in osteosarcoma samples than in paratumor tissues, as shown in Fig. 3b. For analysis of osteosarcoma cells, similar to the histological assay, we examined the differential expression of MALAT1 in hFOB 1.19 cells compared to MG-63 and U2OS cells by RT–qPCR. The results showed that MALAT1 had higher expression in MG-63 and U2OS cells than in hFOB 1.19 cells, as shown in Fig. 3c.

Previous studies have confirmed that MALAT1 promotes biological behaviors such as proliferation and migration in

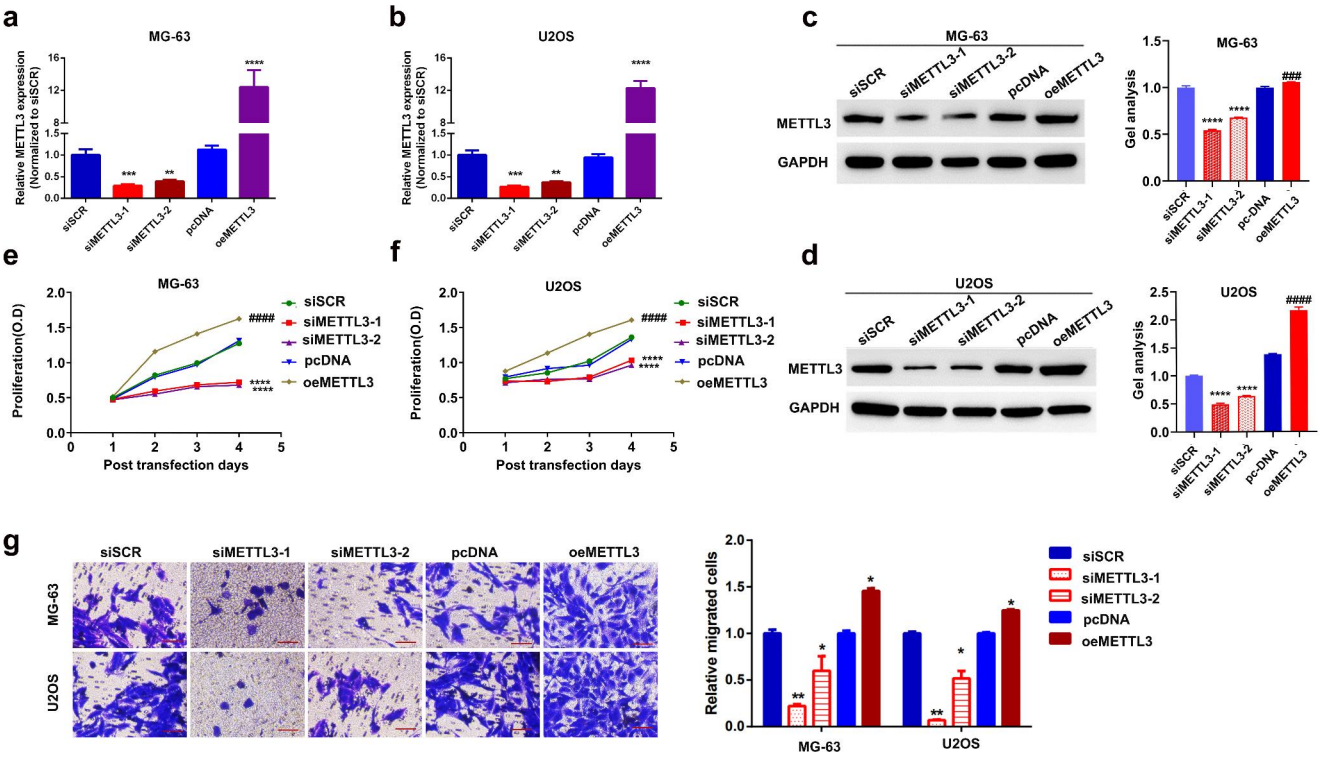

Fig. 2 METTL3 promotes the proliferation and migration of osteosarcoma cells. (a-b) The expression of METTL3 after transfection of specific METTL3 siRNAs or METTL3 overexpression plasmids in MG-63 (a) and U2OS (b) cells was measured by RT–qPCR. $^{**}P<0.01$, $^{***}P<0.001$ and $^{****}P<0.0001$ for si-METTL3-1 and siMETTL3-2 compared to siSCR and for oeMETTL3 compared to pcDNA. (c-d) The expression of METTL3 protein after diverse METTL3 interventions was measured by western blot analysis in MG-63 (c) and U2OS (d) cells. $^{****}P<0.0001$ and $^{\#\#\#\#}P<0.0001$ for si-METTL3-1 and siMETTL3-2 compared to siSCR and for oeMETTL3 compared to pcDNA. (e-f) The growth curve of MG-63 (e) and U2OS (f) cells after diverse METTL3 interventions, as determined by a CCK-8 assay at the indicated times. $^{****}P<0.0001$, $^{\#\#\#\#}P<0.0001$ for si-METTL3-1 and siMETTL3-2 compared to siSCR and for oe-METTL3 compared to pcDNA. (g) Changes in the cell migration ability after diverse METTL3 interventions were evaluated by a Transwell assay. si-METTL3-1 and siMETTL3-2 compared to siSCR and for oeMETTL3 compared to pcDNA. Magnification: 400×; Scale bar: 50 μm. siSCR, scrambled siRNA; siMETTL3-1, METTL3 small interfering RNA-1; siMETTL3-2, METTL3 small interfering RNA-2; oeMETTL3, METTL3 overexpression vector

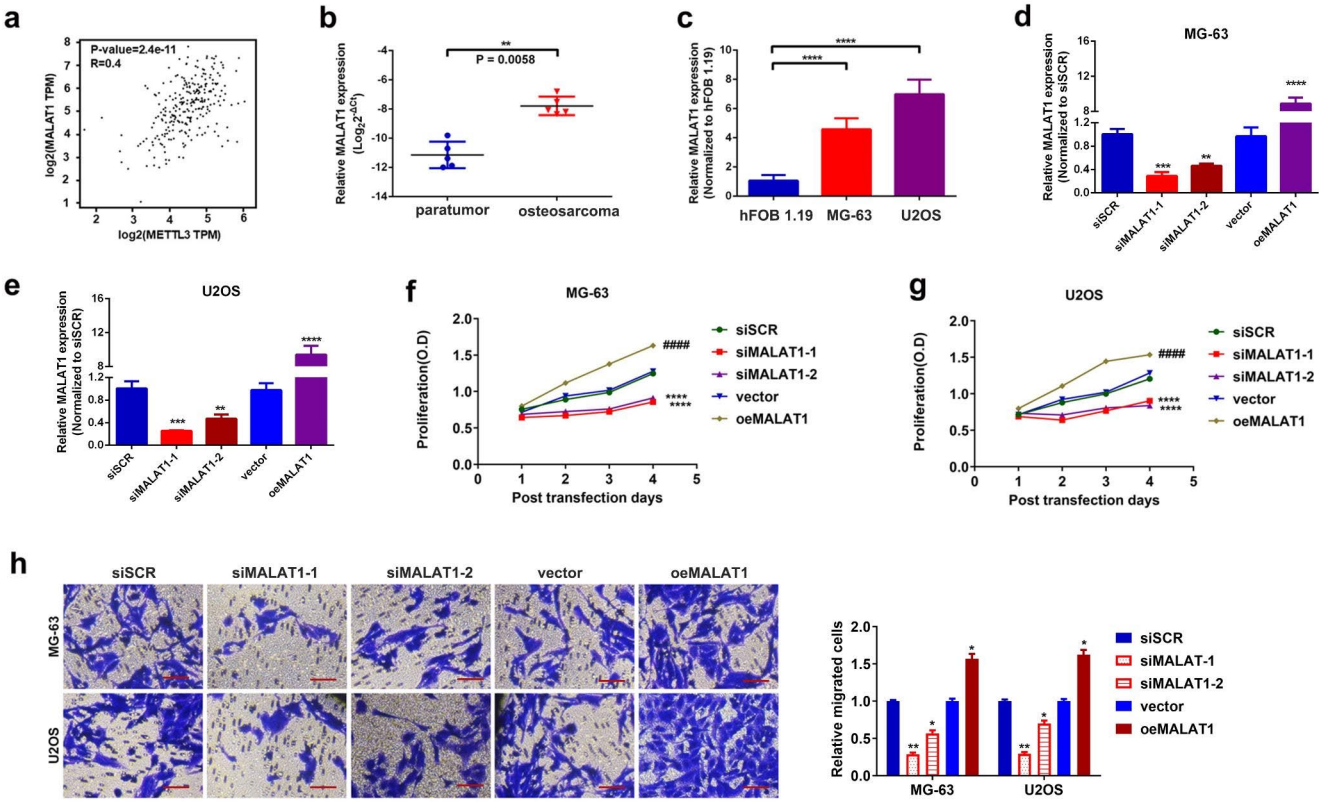

Fig. 3 MALAT1 expression is upregulated and is positively correlated with METTL3 expression in osteosarcoma. (a) The correlation of METTL3 and MALAT1 expression in osteosarcoma samples according to online analysis of TCGA data with UALCAN. $P = 2.4e\text{-}11$, $R = 0.4$ (b) The expression of MALAT1 in 5 collected osteosarcoma tissues and in 5 paired paratumor tissues was measured by RT–qPCR analysis. $^{**}P = 0.0058$ compared with the paratumor group. (c) The expression of MALAT1 in the normal human osteoblast cell line hFOB1.19 and in two osteosarcoma cell lines, MG-63 and U2OS, was measured by RT–qPCR analysis. $^{****}P < 0.0001$ compared with hFOB 1.19. (d-e) The expression of MALAT1 after transfection of specific MALAT1 siRNAs or the MALAT1 overexpression plasmid in MG-63 (d) and U2OS (e) cells was measured by RT–qPCR. $^{**}P < 0.01$, $^{***}P < 0.001$ and $^{****}P < 0.0001$ for si-MALAT1-1 and siMALAT1-2 compared to siSCR and for oe-MALAT1 compared to pcDNA. (f-g) The growth curve of MG-63 (f) and U2OS (g) cells after diverse MALAT1 interventions, as determined by a CCK-8 assay at the indicated times. $^{****}P < 0.0001$, $^{\#\#\#\#}P < 0.0001$, si-MALAT1-1 and siMALAT1-2 compared to siSCR and for oe-MALAT1 compared to pcDNA. (h) Changes in the cell migration ability after diverse MALAT1 interventions were evaluated by a Transwell assay. $^{*}P < 0.05$ and $^{**}P < 0.01$ for si-MALAT1-1 and siMALAT1-2 compared to siSCR and for oe-MALAT1 compared to pcDNA. siMALAT1-1, siSCR, scrambled siRNA; MALAT1 small interfering RNA-1; siMALAT1-2, MALAT1 small interfering RNA-2; Vector, empty vector; oeMALAT1, MALAT1 overexpression vector

osteosarcoma cells [17]. We again confirmed the impact of MALAT1 on the proliferation and migration abilities of MG-63 and U2OS osteosarcoma cells through loss-of-function and gain-of-function assays. We transfected siMALAT1-1 and siMALAT1-2 and siSCR as well as the MALAT1 overexpression plasmid oeMALAT1 and empty vector into MG-63 and U2OS cells. The levels of MALAT1 expression were measured by RT–qPCR, and the results are shown in Fig. 3d-e. The levels of MALAT1 expression in MG-63 and U2OS cells were decreased after transfection with siMALAT1-1 and siMALAT1-2, and the expression levels of MALAT1 in MG-63 and U2OS cells were significantly increased after transfection with oeMALAT1, confirming the successful construction of our cell model. We further investigated the effects of different MALAT1 expression levels on the proliferation and migration abilities of MG-63 and U2OS osteosarcoma cells by CCK8 and Transwell assays. Upregulation of MALAT1 expression significantly promoted MG-63 and U2OS cell proliferation and migration, and downregulation of MALAT1 expression inhibited MG-63 and U2OS cell proliferation and migration (Fig. 3f-h).

METTL3 Functions as an Oncogenic Regulator of Proliferation and Migration in Osteosarcoma by Increasing the Stability of MALAT1

Via the online software SRAMP, we focused on the theoretical m6A modification sites in MALAT1. We found that MALAT1 contained 21 theoretical m6A modification sites (RRACU motifs) (Figure S1). By MeRIP-qPCR analysis, we found that the m6A level of MALAT1 in osteosarcoma

tissues was significantly higher than that in the corresponding paratumor tissues (Fig. 4a). After that, by querying the RMBase database (version 2.0), we found that the exonic region of MALAT1 contains two METTL3 target sites, namely, ModID: m6A_site_77103 and ModID: m6A _site_77104 (Fig. 4b). In MG-63 and U2OS cells, we measured the m6A level of MALAT1 after knockdown of METTL3 by MeRIP-qPCR, and the results are shown in Fig. 4c-d. Compared with that in the siSCR group, the m6A level of MALAT1 was significantly reduced in the siMETTL3-1 and siMETTL-2 groups. Further exploration of the relationship between METTL3-mediated m6A modification and MALAT1 was then conducted. Actinomycin D (2 mg/ml) was added to MG-63 and U2OS cells transfected with si-METTL3 and siSCR, and the half-life of MALAT1 in osteosarcoma cells was determined by RT–qPCR (Fig. 4e-f). The results showed that knockdown of METTL3 significantly decreased the half-life of MALAT1 in MG-63 and U2OS cells. This finding demonstrates that METTL3 can affect the stability of MALAT1 in an m6A-dependent manner.

To further clarify the relationship between MALAT1 and METTL3-mediated promotion of cell proliferation and migration, we first transfected oeMETTL3 into osteosarcoma cells to generate cells with stable overexpression of METTL3, after which specific MALAT1 siRNAs were

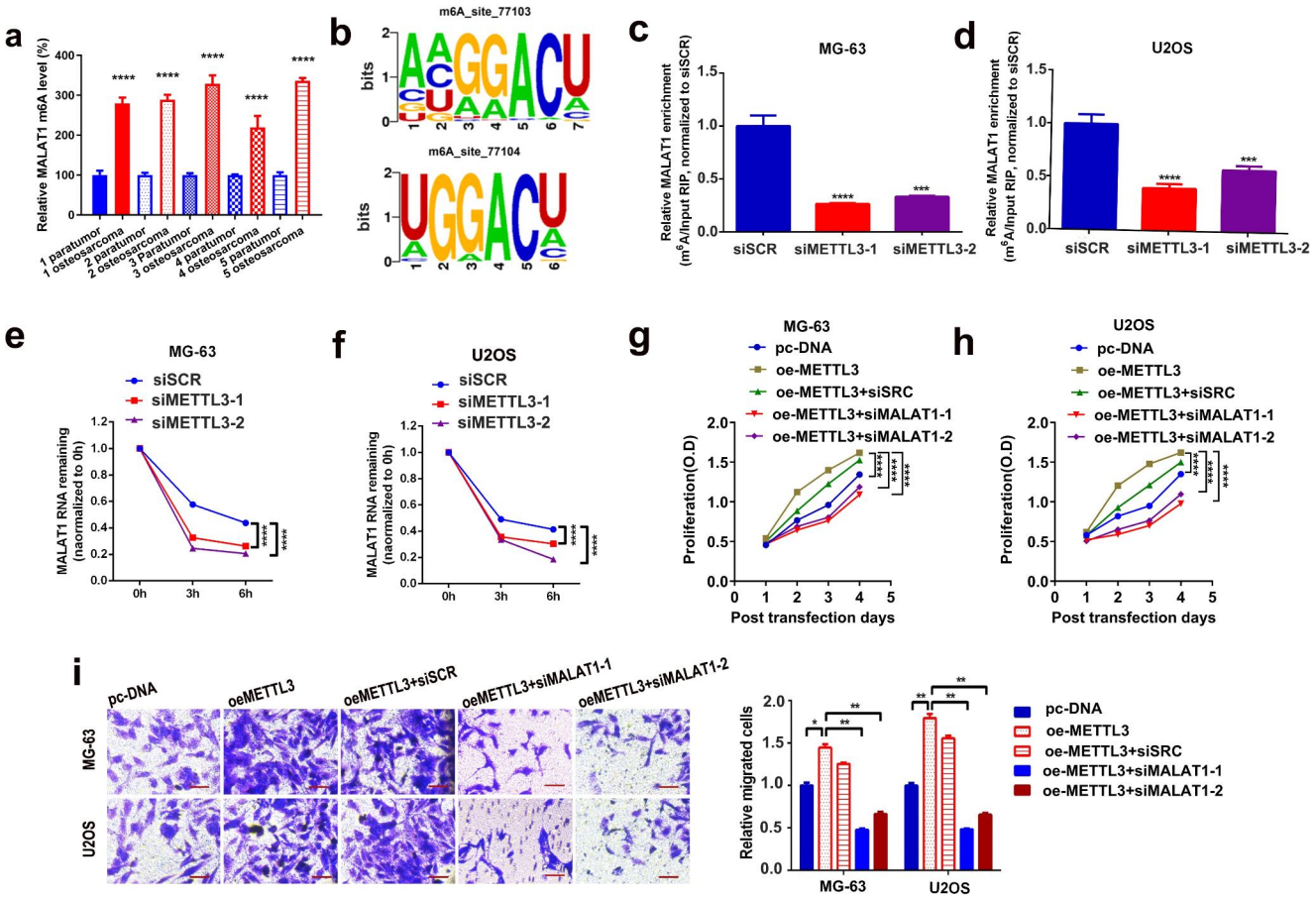

Fig. 4 METTL3 promotes the proliferation and migration of osteosarcoma cells by increasing the stability of MALAT1. (a) The m6A levels of MALAT1 in osteosarcoma tissues were higher than those in paratumor tissues. (n = 5). $^{****}P < 0.0001$ compared with the paratumor group. (b) Details of the 2 METTL3 binding regions in the MALAT1 exon. (c-d) Downregulation of METTL3 decreased the m6A level of MALAT1 in MG-63 (c) and U2OS (d) cells. $^{***}P < 0.001$ and $^{****}P < 0.0001$ compared with siSCR. (e-f) Downregulation of METTL3 decreased the stability of MALAT1 in MG-63 (e) and U2OS (f) cells. $^{****}P < 0.0001$ compared with siSCR. (g-i) After overexpression of METTL3, the growth curves of MG-63 (g) and U2OS (h) cells with different MALAT1 interventions were generated by a CCK-8 assay at the indicated times. $^{****}P < 0.0001$ for oe-METTL3 compared to pcDNA and for oe-METTL3 + siSRC and oe-METTL3 + siMALAT1 compared to oe-METTL3. (i) After overexpression of METTL3, changes in the cell migration ability after diverse MALAT1 interventions were evaluated by a Transwell assay. Magnification: 400×; Scale bar: 50 μm. $^{*}P < 0.05$ and $^{**}P < 0.01$ for oe-METTL3 compared to pcDNA and for oe-METTL3 + siSRC and oe-METTL3 + siMALAT1 compared to oe-METTL3; siSCR, scrambled siRNA; siMETTL3-1, METTL3-specific small interfering RNA-1; siMETTL3-2, METTL3-specific small interfering RNA-2; oeMETTL3, METTL3 overexpression vector; MALAT1 small interfering RNA-1; siMALAT1-2, MALAT1 small interfering RNA-2; Vector, empty vector; oeMALAT1, MALAT1 overexpression vector

transfected into these METTL3-overexpressing MG-63 and U2OS cells. As shown in Fig. 4g-i, the proliferation and migration of MG-63 and U2OS cells were significantly increased after transfection of oeMETTL3 compared to pcDNA, while transfection of siMALAT1-1 or siMALAT1-2 reversed these increases. The results of this assay suggested that silencing MALAT1 reversed the promoting effects of METTL3 on the proliferation and migration of MG-63 and U2OS cells.

Discussion

RNA modifications, documented for over 50 years, have been reported to influence the structure and function of a multitude of RNAs [33]. m6A modification is one of the most common forms of RNA modification and affects various aspects of RNA metabolism, such as pre-mRNA processing, translation efficiency, transcript stability and miRNA biogenesis [34–37]. METTL3 was the first methyltransferase identified and acts as the primary catalyst of m6A modifications on mRNAs and ncRNAs [38, 39]. Recently, the effects of METTL3 have been reported in a number of types of cancer, such as gastric cancer, colon cancer, lung cancer and osteosarcoma [40]. In the current research, via analysis of the GEO and TCGA databases and our experimental validation, we demonstrated that the expression of METTL3 is increased at both the tissue level and cellular level in osteosarcoma, consistent with the results of previous studies [41]. The results of functional CCK8 and Transwell assays indicated that METTL3 was able to promote the proliferation and migration of osteosarcoma cells, demonstrating that METTL3 may act as an oncogenic factor in osteosarcoma.

In recent years, m6A modification of lncRNAs has been extensively studied. Previous studies have revealed that m6A peaks are enriched in lncRNAs [42] and that m6A-modified residues are preferentially located in lncRNA transcripts [43]. Accumulating evidence have indicated that m6A modifications affect the stability of some lncRNAs, such as telomeric repeat-containing RNA (TERRA), growth arrest-specific 5 (GAS5) and Small nucleolar host gene 17 (SNHG17) [44–46]. In the current research, we focused on whether METTL3 was able to increase the stability of MALAT1 in osteosarcoma cells. Bioinformatics analysis revealed a correlation between METTL3 and MALAT1 expression. Subsequently, we found that METTL3 affects the m6A level and half-life of MALAT1. More convincingly, we found that silencing MALAT1 reversed the promotive effects of METTL3 on the proliferation and migration of osteosarcoma cells. All the above findings suggest that MALAT1 is a downstream target of METTL3 in osteosarcoma cells. Notably, knockdown of MALAT1 in cells with METTL3 overexpression resulted in attenuated cell proliferation and migration compared to the control group, demonstrating that there are other regulatory factors acting on MALAT1 to mediate the proliferation and migration of osteosarcoma cells.

The proliferation and metastasis of osteosarcoma cells is a sophisticated and complex biological process involving various pathways, factors and mechanisms. In the present study, we initially determined the expression level of METTL3 in osteosarcoma tissues and cells and confirmed the role of METTL3 in increasing osteosarcoma cell proliferation and migration. LncRNA m6A modification mediated by METTL3 also involves multiple factors; we only preliminarily found that METTL3 could be involved in MALAT1-mediated osteosarcoma cell proliferation and migration through m6A modification, and the specific sites of action of METTL3 and MALAT1 and the involvement of other regulatory factors in the process of m6A modification need to be further investigated.

In summary, the results of our experiments verified that METTL3, acting as an oncogene, was upregulated in osteosarcoma, promoted m6A modification of MALAT1, and increased the stability of MALAT1, thus enhancing MALAT1-mediated oncogenesis. The current study provides a new target for the molecular therapy of osteosarcoma.

Supplementary Information The online version contains supplementary material available at https://doi.org/10.1007/s12033-023-00953-2.

Acknowledgements None.

Authors' Contributions YZ, YX and GQ were responsible for the performance of the experiments; YZ was responsible for the manuscript writing, figure completion and revision of the research. YL, YB, JL and TW were responsible for statistical analysis of the data. YW was mainly responsible for the scientific research and study design.

Funding Statement None.

Data Availability All the data involved in this study are listed.

Declarations

Patient Consent for Publication Not applicable.

Ethical Approval and Consent to Participate The Medical Ethics Committee of Central Hospital Affiliated with Shenyang Medical College approved this study (approval number: 2019DEC12-4), and all patients provided written informed consent.

Competing Interests All authors state the absence of competing interests in the research and writing of the article.

References

1. Moore, D. D., & Luu, H. H. (2014). *Osteosarcoma Cancer Treat Res*, 162: 65–92.
2. Simpson, E., & Brown, H. L. (2018). Understanding osteosarcomas. *Jaapa*, *31*(8), 15–19.
3. Meng, Y., et al. (2021). Circular RNA circNRIP1 plays oncogenic roles in the progression of osteosarcoma. *Mammalian Genome*, *32*(6), 448–456.
4. Ianniello, Z., Paiardini, A., & Fatica, A. (2019). N(6)-Methyladenosine (m(6)A): A Promising New Molecular Target in Acute Myeloid Leukemia. *Frontiers in Oncology*, *9*, 251.
5. Karthiya, R., & Khandelia, P. (2020). m6A RNA methylation: Ramifications for gene expression and Human Health. *Molecular Biotechnology*, *62*(10), 467–484.
6. Meyer, K. D., et al. (2012). Comprehensive analysis of mRNA methylation reveals enrichment in 3' UTRs and near stop codons. *Cell*, *149*(7), 1635–1646.
7. Bokar, J. A., et al. (1997). Purification and cDNA cloning of the AdoMet-binding subunit of the human mRNA (N6-adenosine)-methyltransferase. *Rna*, *3*(11), 1233–1247.
8. Zeng, C., & Huang, W. (2020). *Roles of METTL3 in cancer: Mechanisms and therapeutic targeting*. 13(1): p. 117.
9. Zhang, W., et al. (2020). Multifaceted functions and Novel Insight into the Regulatory Role of RNA N(6)-Methyladenosine modification in Musculoskeletal disorders. *Front Cell Dev Biol*, *8*, 870.
10. Ling, Z., Chen, L., & Zhao, J. (2020). *m6A-dependent up-regulation of DRG1 by METTL3 and ELAVL1 promotes growth, migration, and colony formation in osteosarcoma* Biosci Rep, 40(4).
11. Wang, J., et al. (2022). m6A-dependent upregulation of TRAF6 by METTL3 is associated with metastatic osteosarcoma. *J Bone Oncol*, *32*, 100411.
12. Wei, K., et al. (2022). Methylation recognition protein YTH N6-methyladenosine RNA binding protein 1 (YTHDF1) regulates the proliferation, migration and invasion of osteosarcoma by regulating m6A level of CCR4-NOT transcription complex subunit 7 (CNOT7). *Bioengineered*, *13*(3), 5236–5250.
13. Zhou, C., et al. (2020). N6-Methyladenosine modification of the TRIM7 positively regulates tumorigenesis and chemoresistance in osteosarcoma through ubiquitination of BRMS1. *EBioMedicine*, *59*, 102955.
14. Zhou, X., et al. (2021). METTL3 contributes to Osteosarcoma Progression by increasing DANCR mRNA Stability via m6A modification. *Front Cell Dev Biol*, *9*, 784719.
15. Farzaneh, M., et al. (2023). LncRNA MALAT1-related signaling pathways in osteosarcoma. *Clinical and Translational Oncology*, *25*(1), 21–32.
16. Malakoti, F., et al. (2021). *Multiple function of lncRNA MALAT1 in cancer occurrence and progression*. Chem Biol Drug Des.
17. Wang, Y., et al. (2017). Long non-coding RNA MALAT1 for promoting Metastasis and proliferation by acting as a ceRNA of mir-144-3p in osteosarcoma cells. *Oncotarget*, *8*(35), 59417–59434.
18. Tao, L., et al. (2021). FTO modifies the m6A level of MALAT and promotes Bladder cancer progression. *Oral Diseases*, *11*(2), e310.
19. Li, J., Momen-Heravi, F., & Wu, X. (2023). Mechanism of METTL14 and m6A modification of lncRNA MALAT1 in the proliferation of oral squamous cell carcinoma cells. *Clin Transl Med*, *29*(5), 2012–2026.
20. Jiang, R., et al. (2022). METTL3 stabilizes HDAC5 mRNA in an m(6)A-dependent manner to facilitate malignant proliferation of osteosarcoma cells. *Cell Death Discov*, *8*(1), 179.
21. Zeng, K., et al. (2018). CircHIPK3 promotes Colorectal cancer growth and Metastasis by sponging miR-7. *Cell Death and Disease*, *9*(4), 417.
22. Chen, S., et al. (2019). TCM therapies combined with chemotherapy for preventing recurrence and Metastasis in postoperative II to IIIA NSCLC: A protocol for a systematic review and meta-analysis. *Medicine (Baltimore)*, *98*(9), e14724.
23. Wang, Y., et al. (2018). Long noncoding RNA DANCR, working as a competitive endogenous RNA, promotes ROCK1-mediated proliferation and Metastasis via decoying of mir-335-5p and miR-1972 in osteosarcoma. *Molecular Cancer*, *17*(1), 89.
24. Wang, Y., et al. (2017). Long non-coding RNA TUG1 promotes migration and invasion by acting as a ceRNA of mir-335-5p in osteosarcoma cells. *Cancer Science*, *108*(5), 859–867.
25. Zhou, Y., et al. (2023). Silencing of IRF8 mediated by m6A modification promotes the progression of T-Cell Acute Lymphoblastic Leukemia. *Adv Sci (Weinh)*, *10*(2), e2201724.
26. Ratnadiwakara, M., & Änkö, M. L. (2018). mRNA Stability Assay using transcription inhibition by actinomycin D in mouse pluripotent stem cells. *Bio Protoc*, *8*(21), e3072.
27. Barrett, T., et al. (2013). NCBI GEO: Archive for functional genomics data sets–update. *Nucleic Acids Research*, *41*(Database issue), D991–D995.
28. Chandrashekar, D. S., et al. (2022). UALCAN: An update to the integrated cancer data analysis platform. *Neoplasia (New York, N.Y.)*, *25*, 18–27.
29. Chandrashekar, D. S., et al. (2017). UALCAN: A portal for facilitating Tumor Subgroup Gene expression and survival analyses. *Neoplasia (New York, N.Y.)*, *19*(8), 649–658.
30. Tang, Z., et al. (2019). GEPIA2: An enhanced web server for large-scale expression profiling and interactive analysis. *Nucleic Acids Research*, *47*(W1), W556–w560.
31. Zhou, Y., et al. (2016). SRAMP: Prediction of mammalian N6-methyladenosine (m6A) sites based on sequence-derived features. *Nucleic Acids Research*, *44*(10), e91.
32. Xuan, J. J., et al. (2018). RMBase v2.0: Deciphering the map of RNA modifications from epitranscriptome sequencing data. *Nucleic Acids Research*, *46*(D1), D327–d334.
33. Roundtree, I. A., et al. (2017). Dynamic RNA modifications in Gene expression regulation. *Cell*, *169*(7), 1187–1200.
34. Liu, N., et al. (2015). N(6)-methyladenosine-dependent RNA structural switches regulate RNA-protein interactions. *Nature*, *518*(7540), 560–564.
35. Wang, X., et al. (2015). N(6)-methyladenosine modulates Messenger RNA translation efficiency. *Cell*, *161*(6), 1388–1399.
36. Wang, X., et al. (2014). N6-methyladenosine-dependent regulation of messenger RNA stability. *Nature*, *505*(7481), 117–120.
37. Alarcón, C. R., et al. (2015). N6-methyladenosine marks primary microRNAs for processing. *Nature*, *519*(7544), 482–485.
38. Deng, X., et al. (2018). RNA N(6)-methyladenosine modification in cancers: Current status and perspectives. *Cell Research*, *28*(5), 507–517.
39. Zhao, W., et al. (2020). Epigenetic regulation of m(6)a modifications in Human Cancer. *Mol Ther Nucleic Acids*, *19*, 405–412.
40. Zeng, C., et al. (2020). Roles of METTL3 in cancer: Mechanisms and therapeutic targeting. *Journal of Hematology & Oncology*, *13*(1), 117.
41. Wu, Y., et al. (2022). The role of m6A methylation in osteosarcoma biological processes and its potential clinical value. *Human Genomics*, *16*(1), 12.
42. Han, Y. (2019). *CVm6A: A visualization and exploration database for m6As in cell lines*. *Cells*, 8(2).
43. Zhang, Z., et al. (2021). N6-Methyladenosine-sculpted Regulatory Landscape of noncoding RNA. *Frontiers in Oncology*, *11*, 743990.
44. Chen, L., et al. (2022). METTL3-mediated m6A modification stabilizes TERRA and maintains telomere stability. *Nucleic Acids Research*, *50*(20), 11619–11634.

45. Ni, W., et al. (2019). Long noncoding RNA GAS5 inhibits progression of Colorectal cancer by interacting with and triggering YAP phosphorylation and degradation and is negatively regulated by the m(6)a reader YTHDF3. *Molecular Cancer*, *18*(1), 143.
46. Zhang, H., et al. (2022). m6A methyltransferase METTL3-induced lncRNA SNHG17 promotes lung adenocarcinoma gefitinib resistance by epigenetically repressing LATS2 expression. *Cell Death and Disease*, *13*(7), 657.